

1 **Transient Oxygen Exposure Causes Profound and Lasting Changes to a Benzene-Degrading**
2 **Methanogenic Community**

4 Shen Guo^{1†}, Courtney R. A. Toth^{1†}, Fei Luo^{1‡}, Xu Chen¹, Johnny Xiao¹ and Elizabeth A. Edwards^{1*}

6 ¹Department of Chemical Engineering and Applied Chemistry, University of Toronto, 200 College Street,
7 Toronto, Ontario M5S 3E5, Canada.

8 [†]S.G. and C.R.A.T. contributed equally to this work.

9 ^{*}Current Address: Liven Proteins Corporation, 200 College Street, Toronto, ON M5S 3E5, Canada.

10 *Corresponding Author: Elizabeth A. Edwards., e-mail: elizabeth.edwards@utoronto.ca; Tel. (+1) 416
11 946 3506; Fax (+1) 416 978 8605.

12

13

14 **DETAILS OF AUTHOR AFFILIATIONS**

15 Shen Guo – Department of Chemical Engineering and Applied Chemistry, University of Toronto, Toronto,
16 Ontario M5S 3E5, Canada.

17 Courtney R. A. Toth – Department of Chemical Engineering and Applied Chemistry, University of
18 Toronto, Toronto, Ontario M5S 3E5, Canada; orcid.org/0000-0003-3430-0792.

19 Fei Luo – Department of Chemical Engineering and Applied Chemistry, University of Toronto, Toronto,
20 Ontario M5S 3E5, Canada; Present Address: Liven Proteins Corporation, 200 College Street, Toronto, ON
21 M5S 3E5, Canada.

22 Xu (Charlie) Chen – Department of Chemical Engineering and Applied Chemistry, University of Toronto,
23 Toronto, Ontario M5S 3E5, Canada.

24 Johnny Xiao – Department of Chemical Engineering and Applied Chemistry, University of Toronto,
25 Toronto, Ontario M5S 3E5, Canada.

26 Elizabeth A. Edwards – Department of Chemical Engineering and Applied Chemistry, University of
27 Toronto, Toronto, Ontario M5S 3E5, Canada; orcid.org/0000-0002-8071-338X.

28 **ABSTRACT**

29 We investigated the impact of oxygen on a strictly anaerobic, methanogenic benzene-degrading
30 enrichment culture derived decades ago from oil-contaminated sediment. The culture includes a
31 benzene fermenter from Deltaproteobacteria Candidate clade Sva0485 (referred to as ORM2) and
32 methanogenic archaea. A relatively small one-time injection of air, simulating a small leak into a batch
33 culture bottle, had no measurable impact on benzene degradation rates, although retrospectively, a tiny
34 enrichment of aerobic taxa was detected. A subsequent 100 times larger injection of air stalled
35 methanogenesis and caused drastic perturbation of the microbial community. A benzene-degrading
36 *Pseudomonas* became highly enriched and consumed benzene and all available oxygen. Anaerobic
37 benzene-degrading ORM2 cell numbers plummeted during this time; re-growth and associated recovery
38 of methanogenic benzene degradation took almost one year. These results highlight the oxygen-
39 sensitivity of this methanogenic culture and confirm that the mechanism for anaerobic
40 biotransformation of benzene is independent of oxygen, fundamentally different from established
41 aerobic pathways, and is carried out by distinct microbial communities. The study further highlights the
42 importance of including microbial decay in characterizing and modelling and mixed microbial
43 communities.

44

45 **KEYWORDS**

46 Benzene, anaerobic, bioremediation, methanogenesis, oxygen, *Pseudomonas*, cell decay

47

48 **SYNOPSIS**

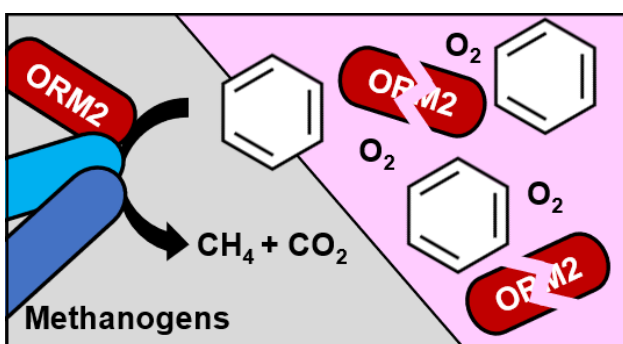
49 Methanogenic benzene degradation in a highly enriched anaerobic consortium was inhibited for a year
50 after transient exposure to oxygen, causing mass decay of benzene-fermenting bacteria.

51

52 **GRAPHIC FOR ABSTRACT ART**

53

54



55 **INTRODUCTION**

56 Benzene is a widespread and toxic pollutant notorious for its persistence in anaerobic environments
57 including contaminated aquifers and deep sediments. Once thought to be completely recalcitrant in the
58 absence of molecular oxygen, four decades of research now support the contrary. Anaerobic
59 transformation of [¹⁴C] benzene to labelled CO₂ was first documented in studies in the aftermath of the
60 Amoco Cadiz oil spill in 1980 (Ward et al., 1980). Years later, this methanogenic activity was reproduced
61 in several laboratory-scale experiments (Vogel and Grbić-Galić, 1986; Wilson et al., 1986; Grbić-Galić and
62 Vogel, 1987; Kazumi et al., 1997; Weiner and Lovley, 1998). Oxidation of [¹⁴C] benzene to labelled CO₂
63 was also stoichiometrically linked to the reduction of ferric iron (Coates et al., 1996; Holmes et al.,
64 2011), nitrate (Burland and Edwards, 1999; Chakraborty et al., 2005) and sulfate (Edwards and Grbić-
65 Galić, 1992; Lovley et al., 1995; Coates et al., 1996; Phelps et al., 1996; Kazumi et al., 1997), catalyzed by
66 a handful of specialized microorganisms in enrichment cultures as reviewed in Vogt et al. (2011) and
67 Toth et al. (2021). Although an enzymatic mechanism for anaerobic benzene activation has still not been
68 established, proposed oxygen-independent transformation reactions include hydroxylation (Vogel and
69 Grbić-Galić, 1986; Caldwell and Suflita, 2000; Zhang et al., 2013), carboxylation (Caldwell and Suflita,
70 2000; Kunapuli et al., 2008; Abu Laban et al., 2010; Luo et al., 2014), or activation to benzoyl-CoA
71 involving Wood-Ljungdahl pathway intermediates (Devine, 2013). The existence of at least two different
72 activation mechanisms is predicted from stable isotope fractionation experiments (Mancini et al., 2008).
73

74 Benzene biodegradation proceeds more readily under aerobic conditions (Atlas, 1981) and is usually
75 preferred for bioremediation applications. In the subsurface, the caveat becomes supplying enough
76 oxygen to drive complete benzene attenuation. Low permeability contaminated aquifers rapidly deplete
77 dissolved O₂, creating anaerobic zones where benzene remains recalcitrant. In situ injection of oxygen is
78 inefficient, as O₂ is poorly soluble in water and demand from contaminants and other reduced species is
79 large. Other technologies such as traditional excavation or pump-and-treat strategies are costly and
80 disruptive to the site, and not always feasible at large or deep sites. Recent studies have proposed
81 injecting other agents such as nanoparticles (e.g., metal peroxides, zero valent iron) into the zone of
82 contamination (Otto et al., 2008; Lu et al., 2017; Galdames et al., 2020), but these can be limited by
83 difficulties in distribution, aggregation, maintaining activity and cost. In the end, anaerobic
84 bioremediation may be a more economical and sustainable strategy for such locations. Decontamination
85 can be achieved anaerobically by encouraging the growth of certain native microorganisms which can
86 degrade contaminants (biostimulation) or by adding exogenous culture (bioaugmentation) (Reinhard et
87 al., 1997; Cunningham et al., 2001; Major et al., 2002; Löffler and Edwards, 2006; Toth et al., 2021).
88

89 Perhaps ironically, one of the questions we are most frequently asked is if successful benzene
90 bioremediation can truly be independent of oxygen. This skepticism is in part due the chemical stability
91 of its unsubstituted aromatic ring and the long history of difficulties cultivating anaerobic benzene-
92 degrading cultures (Meckenstock et al., 2016). Several reports of oxygen-generating reactions in an
93 otherwise anoxic environment also contribute to this apprehension (Bruce et al., 1999; Weelink et al.,
94 2008; Mehboob et al., 2009; Ettwig et al., 2010; Atashgahi et al., 2018). For example, nitrate and
95 chlorate dismutation reactions have been shown to generate molecular oxygen internally that can then
96 be used in benzene activation with powerful O₂-dependent oxygenases (Weelink et al., 2008;
97 Oosterkamp et al., 2013; Atashgahi et al., 2018). However, mono- and dioxygenase genes and associated
98 aerobic pathways have never been detected in the metagenomes of some benzene-degrading anaerobic
99 cultures (Abu Laban et al., 2010; Devine, 2013; Luo et al., 2014; Luo et al., 2016). Others have suggested
100 that reactions with iron can generate radical oxygen species that may oxidize benzene (Kunapuli et al.,
101 2008). While this can occur, it's highly unlikely to drive benzene degradation at consistent rates and
102 stoichiometry indefinitely, especially in longstanding enrichment cultures (Luo et al., 2014; Luo et al.,

103 2016; Toth et al., 2021).

104

105 The objective of this study was to understand how the input of a little bit of oxygen into an active
106 methanogenic benzene-degrading enrichment culture would affect degradation rates and impact its
107 microbial community composition. This enrichment culture and its key benzene-degrading fermenter
108 (ORM2, an unclassified member of the Deltaproteobacteria Candidate clade Sva0485) was recently
109 described in detail in Toth et al. (2021). Nearly identical 16S rRNA gene sequences to ORM2 were also
110 found in benzene-degrading methanogenic cultures from Japan (Sakai et al., 2009; Noguchi et al., 2014)
111 and in microcosms from China (Qiao et al., 2018). From our results we determined that addition of
112 oxygen stimulated the growth of a benzene-degrading *Pseudomonas* that was undetectable in the
113 culture prior to oxygen exposure. Furthermore, oxygen addition resulted in dramatic reductions in
114 ORM2 cell numbers and declines of other bacteria and archaea that are vital to this culture. Recovery of
115 methanogenic benzene degradation took almost an entire year after anoxic conditions were re-
116 established, attributed to the rapid decay of ORM2 cells and subsequent long doubling times to re-
117 establish initial (pre-oxygen) concentrations. These data clearly refute any possible involvement of
118 oxygen in benzene activation by ORM2.

119

120 MATERIALS AND METHODS

121 **Methanogenic benzene-degrading culture DGG-B.** DGG-B is a large-scale culture lineage derived from
122 the lab-scale methanogenic benzene-degrading consortium OR, established over 20 years ago from site
123 materials from an oil refinery in Oklahoma, USA (Nales et al., 1998; Toth et al., 2021). Large scale DGG-B
124 cultures are grown at SiREM laboratories (Guelph, ON) in 100-L stainless steel vessels containing a
125 defined anaerobic, mineral medium (Ulrich and Edwards, 2003) and benzene as their sole carbon and
126 energy source (aqueous concentration of 25 mg/L, approximately 32 mmol per vessel) added every 4-6
127 weeks or as needed. The growth medium contains amorphous iron sulfide (FeS) as a reducing agent and
128 resazurin as a redox indicator. DGG-B is currently undergoing bench-scale and field-scale testing to
129 evaluate its potential for bioaugmentation of benzene-contaminated groundwater (Toth et al., 2021).

130

131 **Experimental setup and sampling.** In May 2017, an aliquot (~1 L) of DGG-B was transported in a sealed
132 bottle from SiREM labs to the University of Toronto for testing. Culture portions (30 mL) were dispensed
133 into twenty-three 40 mL clear glass screw-cap bottles and amended with neat benzene (4.1
134 $\mu\text{mol}/\text{bottle}$) for an initial aqueous concentration of 10 mg/L. Bottles were sealed with Teflon Mininert
135 screw caps and incubated in a Coy anaerobic glovebox (supplied with 10% H_2 , 10% CO_2 , and 80% N_2) at
136 room temperature (~23 °C). Benzene depletion and methane formation was monitored and bottles were
137 reamended with benzene when concentrations dropped below 5 mg/L. After ~9 months of monitoring
138 all the bottles, five bottles (designated Bottles 1 – 5) with similar and consistent benzene degradation
139 rates (~0.3 $\mu\text{mol}/\text{bottle}/\text{day}$ or about 0.8 mg/L/day) were selected for inclusion in this oxygen tolerance
140 experiment.

141

142 Experimental treatments for each bottle are provided in Table 1. Day 0 of the experiment was March
143 19th, 2018, when each of the 5 similar bottles was refed and closer monitoring began. Bottles 1 to 3
144 were amended with an initial 0.1 mL dose of room air (~78% N_2 and 21% O_2) on Day 39 or 53 of this
145 experiment by syringe injection. Subsequently, Bottles 1 and 2 received one (Bottle 1, Day 94) or two
146 successive (Bottle 2, Days 94 and 224) additional doses of approximately 10 mL air (Table 1), achieved by
147 opening (for 15 s) and closing the bottle cap to replace the headspace volume with air. As illustrated in
148 Figure 1, the addition of 10 mL air made the resazurin in the culture medium turn pink (oxidized form).
149 Once the resazurin returned to its colourless (reduced) form, we assumed all available O_2 was depleted.
150 Two bottles served as positive controls (Bottles 4 and 5) that were maintained in the glovebox as usual

151 and never exposed to oxygen. Bottle 6 (medium only) was prepared as an anaerobic sterile control that
152 was then exposed to 10 mL air on Day 16. Active bottles were incubated for up to 1225 days.

153

154 **DNA extraction and molecular analyses.** Bottles 1 – 5 were routinely sampled for molecular analyses.
155 Cell pellets (10,000 × g centrifugation, 15 min) from 1 mL of culture were frozen at -80 °C for later DNA
156 extraction using the DNeasy PowerSoil Kit (Qiagen) according to the manufacturer's procedure.
157 Concentrations of extracted DNA were verified using a Nanodrop ND-1000 spectrophotometer (Thermo
158 Fisher Scientific).

159

160 DNA samples were assayed by quantitative PCR (qPCR) using previously established primer pairs for
161 total Bacteria, total Archaea, ORM2, and *Candidatus* Nealsonbacteria (previously referred to as OD1 and
162 Parcubacteria, Table S1). Amplification of targeted genes was carried out in duplicate 20 µL reactions
163 containing 10 µL of SsoFast™ EvaGreen® Supermix (Bio-Rad Laboratories, Hercules, CA), 2 µL of DNA
164 template, 500 nM of each designated forward and reverse primer, and UV-treated UltraPure distilled
165 water (Thermo Fisher Scientific). Serial dilutions of plasmids containing corresponding 16S rRNA gene
166 fragments were used to generate standard curves. qPCR reactions were performed using a CFX96 real-
167 time thermal cycler (Bio-Rad Laboratories) using the following thermocycling conditions: an initial
168 denaturation step at 98 °C for 2 min, 40 cycles of 98 °C for 5 s and T_m (see Table S1) for 10 s, followed by
169 melt curve analysis (65–95 °C with an increase of 0.5 °C every 5 s). qPCR results were processed with CFX
170 Manager software (Bio-Rad Laboratories).

171

172 Finally, aliquots of DNA extracts were shipped on dry ice to the Genome Quebec Innovation Centre for
173 Illumina MiSeq 300PE (paired-end) 16S rRNA amplicon sequencing. All amplicon sequence reads were
174 generated using modified, “staggered end” 16S rRNA gene primers 926F and 1392R (Table S1) as
175 previously described in Toth et al. (2021). Read processing and sequencing analyses were performed in
176 QIIME 2 version 2020.11 (Callahan et al., 2016). The SILVA SSU 132 database (Quast et al., 2013) was
177 used to classify the resulting amplicon sequence variants (ASVs). ASVs with the same taxonomy are
178 ranked by abundance, where ASV1 is the most abundant sequence variant recovered across all DNA
179 samples. Two sequence variants (ASV IDs c0bc311ae7b8da92ad4208a5c83926bf and
180 29ca2edb9ec3825021ea0fc78298c83c) were reclassified from *Ca. Yanofskybacteria* to *Ca.*
181 *Nealsonbacteria* based on matching nucleotides sequences to a complete (closed) genome recovered
182 from the DGG-B/OR consortium (Chen et al., data in preparation; closed genome of *Ca. Nealsonbacteria*
183 available in JGI/IMG, taxon ID 2791354853). Raw amplicon sequence reads were deposited to the
184 National Center for Biotechnology Short Read Archive (SRA) under BioProject PRJNA807302.

185

186 **Analytical procedures.** Headspace samples (300 µL) from experimental bottles were injected into a
187 Hewlett-Packard 5890 Series II gas chromatograph equipped with GSQ 30 m × 0.53 mm I. D. PLOT
188 column (J & W Scientific) and a flame ionization detector (GC-FID) to quantify benzene and methane as
189 previously described (Luo et al., 2016). Benzene and methane concentrations were monitored over time
190 in Bottles 1 – 6, from before exposure to air until after anaerobic benzene degradation resumed; all data
191 are provided in Table S2.

192

193 **Microbial data analysis.** Results of qPCR analyses of absolute abundances of targeted microbial groups
194 (16S rRNA gene copies per mL culture) and overall community composition (from 16S rRNA gene
195 amplicon sequencing) are summarized in Tables S3 and S4a to S4d. We also estimated the absolute
196 abundance of all bacterial or archaeal amplicon sequence variants (ASV) detected in this study by taking
197 the total absolute bacterial or archaeal abundance by qPCR multiplied by the relative abundance within
198 each Domain from amplicon sequencing (Tables S5 and S6). Abundances measured using taxon-specific

199 qPCR were similar to abundance estimated from multiplying general bacteria or archaea qPCR results by
200 the relative abundance obtained from amplicon sequencing. Concentrations (in 16S rRNA gene
201 copies/mL over time) for most abundant ASVs in select bottles are highlighted in main text figures
202 (Figures 2 and 3) and for all other active bottles and major ASVs in Supplementary Figures. The amplicon
203 sequence of one ASV of interest (*Pseudomonas* ASV1, 466 bp) was used to build a maximum likelihood
204 tree in Geneious 8.1.9 using a GTRGAMMA model and 100 bootstrap replicates.
205

206 RESULTS AND DISCUSSION

207 **Methanogenic benzene degradation and microbial growth in bottles not exposed to oxygen.** DGG-B
208 cultures in Bottles 4 and 5 were maintained as usual in the anaerobic glovebox, without exposure to
209 oxygen. Benzene was repeatedly degraded throughout the monitoring period, with a gradual increase in
210 rate from 0.8 mg/L/day to 6 mg/L/day over 422 days (Figures 2a and S1a). In the first 200 days, the ratio
211 of methane produced to benzene consumed averaged 3.5 ± 0.1 mol/mol (Table S2), nearly identical to
212 the expected stoichiometry shown in Equation 1, where benzene (C_6H_6) is converted to methane (CH_4),
213 CO_2 and cells ($C_5H_7O_2N$). Similar ratios have been previously reported for consortia maintained in our
214 laboratory (Ulrich and Edwards, 2003; Luo et al., 2016) and elsewhere (Kazumi et al., 1997; Sakai et al.,
215 2009). After 200 days, measured methane concentrations began to plateau and were underestimated
216 due to pressure buildup and associated losses from sampling.
217

218 Equation 1: $C_6H_6 + 3.9 H_2O + 0.15 NH_4^+ + 0.15 HCO_3^- \rightarrow 3.375 CH_4 + 2.025 CO_2 + 0.15 C_5H_7O_2N$
219

220 Dominant microbial phylotypes in the DGG-B/OR consortium include Deltaproteobacteria Candidate
221 clade Sva0485 (ORM2), acetoclastic *Methanosaeta* and hydrogenotrophic *Methanoregula* that are
222 required for complete biodegradation of benzene to CH_4 and CO_2 (Devine, 2013; Luo et al., 2016; Toth et
223 al., 2021). A member of the Candidate Phyla Radiation (*Ca. Nealsonbacteria*, previously referred to as
224 OD1 and Parcubacteria) has also been consistently found in the culture (Luo et al., 2016; Toth et al.,
225 2021) and is thought to be involved in biomass recycling (Chen et al., data in preparation). Absolute
226 abundance was tracked by qPCR and is shown in Figure 2b (Bottle 4) and Figure S1b (Bottle 5). Turning
227 next to 16S rRNA gene amplicon sequencing, three ASVs increased the most; Sva0485
228 Deltaproteobacteria ASV1 (ORM2), *Methanosaeta* ASV1, and *Methanoregula* ASV1 (Figures 2c and S1c;
229 Tables S5 and S6). Other high abundance ASVs belonged to *Ca. Nealsonbacteria* and *Ca. Omnitrophica*
230 (previously referred to as OP3), a candidate phylum that may also be implicated in biomass recycling
231 (Suominen et al., 2021)(Figures 2c and S1c; Tables S3 and S5). Overall, the observed benzene
232 degradation rates and growth of ORM2, methanogens and candidate phyla were as expected in these
233 positive control bottles.
234

235 **Benzene biodegradation following oxygen exposure.** In experimental bottles, the impacts of exposure
236 to oxygen are illustrated in Figure 3a (Bottle 2), Figures S2a and S3a (Bottles 1 and 3), and summarized in
237 Table 1. After the first addition of 0.1 mL air, the culture medium remained clear, indicating that the
238 resazurin remained reduced. There was also no observable impact on benzene degradation rate or
239 methane production, as seen by the data from Bottle 3 (Figure S3). We surmised that the FeS used to
240 reduce the culture medium (15 μ mol/bottle) scavenged the added O_2 (~0.9 μ mol/bottle) and that
241 exceeding the oxygen demand from FeS (34 μ mol/bottle) would be necessary to elicit a change in
242 benzene degradation activity (calculations shown in Table S7). The headspace volume of the bottles was
243 10 mL. We reasoned that if we simply opened the bottle cap for a few seconds and then closed it, we
244 would effectively replace the headspace volume with air. Using this approach, we added ~10 mL of air
245 (~86 μ mol/bottle of O_2) once to Bottle 1, twice to Bottle 2, and once to medium-only (sterile) Bottle 6

246 (Table 1). Expectedly, the culture medium immediately turned pink and remained pink for up to 70 days
247 in live replicates (Figures 3a, S2a, and S4). No methane production was observed when the bottles were
248 still pink. Benzene degradation was able to proceed in Bottles 1 and 2 following a brief lag period (~1
249 week) but stopped after 61 – 70 days, coinciding with oxygen depletion (when the resazurin turned clear
250 again). After adding a second 10 mL of air to Bottle 2, benzene degradation resumed for 35 days until O₂
251 was depleted once again (Figure 3a). No benzene loss was detected in Bottle 6 after oxygen was added
252 (Figure S4), indicating that the benzene losses seen in Bottles 1 and 2 were not the result of
253 contamination from added air. A moles balance comparing benzene degraded during the aerobic “pink”
254 period to the amount of available oxygen in each bottle confirmed that observed benzene depletion
255 after adding air to the bottles was coupled to oxygen consumption (Table S7).

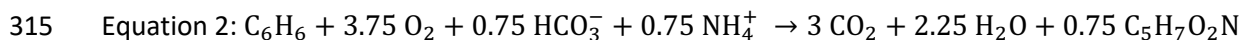
256
257 We continued to monitor these bottles to determine if and when anaerobic benzene degradation would
258 re-establish. Methane production began slowly over several months, and finally methanogenic benzene
259 degradation was measurable again by Day 583 in Bottle 1 and by Day 666 in Bottle 2 (Figures 3a and S2a;
260 Table 1). This lag of 323-325 days was much longer than expected, even considering the known, slow
261 doubling time of ~30 days for ORM2 (Ulrich and Edwards, 2003; Luo et al., 2016; Toth et al., 2021). This
262 prompted us to take a closer look at the microbes in each bottle over time.

263
264 **Appearance of *Pseudomonas* upon exposure to oxygen.** Our amplicon sequencing data immediately
265 revealed that an ASV affiliated with *Pseudomonas* became highly enriched in Bottles 1 and 2 after
266 adding 10 mL of air (Figures 3b, 3c, S2b, and S2c). Using Bottle 2 as an example, we can see
267 concentrations of *Pseudomonas* ASV1 copies/mL increased rapidly in the presence of oxygen (up to 1.2 ×
268 10⁹ copies/mL) but decayed very slowly under anoxic conditions (Figure 3b). It took until Day 1207 for
269 concentrations of *Pseudomonas* ASV1 to fall below detectable limits. Looking closely at Bottle 3, we can
270 see transient, low abundances of *Pseudomonas* ASV1 appear after the first 0.1 mL injection of air, even
271 though no perturbation of the culture was observed (Figure S3b). *Pseudomonas* have not previously
272 been detected in the DGG-B/OR consortium (Ulrich and Edwards, 2003; Luo et al., 2016; Toth et al.,
273 2021) and no ASVs associated with *Pseudomonas* were ever detected in anoxic controls Bottles 4 and 5
274 (Table S4a). This ASV was likely not a contaminant from the air or growth medium used because
275 benzene losses were never detected in medium-only control Bottle 6 (Table 1; Figure S4). *Pseudomonas*
276 ASV1 is closely related (100% sequence identity) to several *Pseudomonas stutzeri* isolates (Figure S5),
277 although a longer 16S rRNA gene sequence (>466 base pairs) or genome is needed to verify taxonomy.
278 *P. stutzeri* species are metabolically versatile and can use oxygen or nitrate as a terminal electron
279 acceptor (Lalucat et al., 2006). A handful of strains are also capable of mineralizing aromatic
280 hydrocarbons (Grimberg et al., 1996; Ortega-Calvo et al., 2003; Heinaru et al., 2016). Considering the
281 above analysis, benzene-degrading *Pseudomonas* likely persist below detection in the DGG-B culture
282 and were responsible for the aerobic benzene metabolism seen in Bottles 1 and 2 (Figures 3a and S2a).

283
284 **Impact of oxygen on ORM2 and methanogens.** The community composition and absolute abundance
285 of ORM2, Archaea and Bacteria tracked in anoxic controls Bottles 4 and 5 provide a reference against
286 which oxygen-impacted Bottles 1 – 3 were compared(Figures 2, 3, S1-S3). Prior to oxygen addition,
287 concentrations of ORM2 in Bottle 3 (~9.5 × 10⁷ copies/mL) were comparable to those measured in
288 anoxic control Bottles 4 and 5 (Table S3). After adding 10 mL of air to Bottles 1 and 2, concentrations of
289 ORM2 steeply decreased by up to 2 orders of magnitude (Figures 3b and S2b). The addition of only 0.1
290 mL of air in Bottle 3 may even have resulted in a small (~53%) decrease in concentrations of ORM2
291 (Table S3). We were surprised to see that ORM2 concentrations continued to decline in Bottles 1 and 2
292 long after the bottles were no longer pink and presumed to be devoid of O₂. The lowest concentrations
293 of ORM2 measured were 2.9 × 10⁶ copies/mL on Day 401 in Bottle 1 (Figure S2b) and 2.0 × 10⁵

294 copies/mL on Day 401 in Bottle 2 (Figures 3b). Both concentrations are below estimated threshold
295 concentrations of ORM2 (4.3×10^6 ORM2 copies/mL) needed for measurable benzene loss in batch
296 cultures of DGG-B (Toth et al., 2021). Concentrations of total Archaea also declined up to 1 order of
297 magnitude between Days 98 – 585 (Figures 3b and S2b). While ORM2 abundance decreased, the
298 abundance of total Bacteria increased by 56-80% immediately after adding 10 mL of air (Tables S3 and
299 S5), driven by the growth of aforementioned *Pseudomonas*. After the medium in Bottles 1 and 2 turned
300 clear, *Pseudomonas* copies began to decrease yet it still took a further 140-240 days to see net increases
301 in ORM2 copies. This prompted us to take a closer look at observed growth and decay rates. Transient
302 oxygen exposure had a prolonged negative impact on the microbial community structure of DGG-B.
303

304 **Estimates of cell yields, growth and decay rates for *Pseudomonas* and ORM2.** We performed mass and
305 electron balances in each bottle to compare the ratios of donor (benzene) consumption to oxygen
306 reduction (in aerobic phases) and to methane formation (in anoxic phases), including biomass
307 formation. Cell yields were estimated from qPCR (16S rRNA gene copies/mL), cell size (g/copy), and
308 benzene consumption data over each time interval; these calculations are detailed in Table S8. Although
309 qPCR can overestimate cell copy numbers by capturing DNA from dead cells (Kralik and Ricchi, 2017), we
310 assumed this risk to be minimal since cell decay on the orders of magnitude were observed in this study.
311 Measured values were compared to predictions shown in Equation 1 (methanogenic case) and in
312 Equation 2 (aerobic case). In Equation 2, the fraction of electrons from benzene going to cell synthesis
313 was 50% which is typical for aerobic processes (Rittmann and McCarty, 2001).
314



317 The average measured yield for *Pseudomonas* (~1.1 g cells per g of benzene) during the aerobic phase
318 was remarkably close the predicted yield (Table 2). In contrast, the total yield of ORM2 and total
319 Archaea under methanogenic conditions (~0.04 g cells/g benzene) was found to be well below predicted
320 growth yield (0.22 g/g) shown in Equation 1 and in Table 2. Low growth yields have been previously
321 reported for this culture (Luo et al., 2016; Toth et al., 2021) and are consistent with the difficulties
322 commonly reported in trying to sustain high rates and cell concentrations in anaerobic benzene-
323 degrading cultures.
324

325 To explore growth and decay rates more closely, we estimated net (*i.e.*, measured) cell growth and
326 decay rates for the two benzene degraders, *Pseudomonas* and ORM2 (Table S8), assuming first order
327 processes as an approximation. Using the slope from first order regression of microbial abundance (from
328 qPCR) vs time over specific intervals (aerobic, anaerobic), we were able to get some estimates that
329 reflect observations in Bottles 1 – 5 (Table S8). In Table 2, we summarize the average and fastest rates
330 estimated and provide calculated, representative doubling times or half-lives to make comparisons
331 easier.
332

333 Growth rates for *Pseudomonas* were substantially faster than for ORM2, best seen in Table 2 by the
334 difference in minimum/average doubling times (6/9 days vs 26/66 days, respectively). These data are
335 consistent with literature and previous reports for ~30 day doubling times for ORM2 (Ulrich and
336 Edwards, 2003; Luo et al., 2016; Toth et al., 2021). As for observed decay rates, we see striking numbers
337 for ORM2, particularly during aerobic phases where the fastest decay rates and shortest half-lives of
338 only 11 days were reported (Table 2, Table S8). This highlights a substantial loss of ORM2 biomass upon
339 exposure to oxygen. The average half-life of ORM2 (calculated during aerobic and anaerobic periods of
340 decay) was about 38 days, which is very short and incredibly close to the organism's known doubling
341 time. Therefore it is not surprising that it took almost a year for the culture to recover. In previous

342 experiments by Luo et al. (2016), decay was essentially zero for ORM2 maintained anaerobically and
343 without benzene. ORM2 is thus highly sensitive to oxygen and reinforces the existence of a novel, still
344 unknown pathway independent of O₂ in methanogenic benzene degradation.

345

346 **Impact of oxygen on other microbial community members.** After realizing just how sensitive ORM2 is
347 to oxygen, we were curious how other members of the DGG-B community responded to air addition
348 events. Putative microbes represented by ASVs were divided into Bacteria and Archaea and further
349 categorized into one of three groups; i) ASVs that became enriched aerobically, ii) ASVs that declined in
350 response to O₂ exposure, and iii) ASVs that were largely unaffected (Figures S6a – S6d and S7a – S7d).

351

352 Group 1 Bacteria that were positively impacted by oxygen include the *Pseudomonas* ASV1 discussed
353 above, as well as *Sulfurferula* ASV1, *Thiomonas* ASV1, and *Rhizobium* ASV1 (Figures S6aS6b and S6c).
354 None of these ASVs were detectable in anoxic control Bottles 4 and 5 at any time point (Figure S6d).
355 Members of these genera are aerobic but can survive under anoxic conditions (Vela et al., 2002; Lalucat
356 et al., 2006; Watanabe et al., 2015; 2016). *Sulfurferula* and *Thiomonas* are chemolithoautotrophs that
357 oxidize some sulfur species (S⁰, thiosulfate, sulfide, and tetrathionate) with O₂ (Watanabe et al., 2015;
358 2016). The FeS reducing agent in our growth medium could logically have supported the growth of
359 *Sulfurferula* ASV1 or *Thiomonas* ASV1 in the presence of O₂. In our electron balance, we assumed the
360 oxidation of FeS was abiotic but these data suggest it may instead have been biotic. Select rhizobial
361 species can metabolize substituted aromatics including phenol, a hydroxylated form of benzene that can
362 be produced abiotically by autoxidation (Vela et al., 2002; Kunapuli et al., 2008).

363

364 Group 2 microbes that were negatively impacted by oxygen include those we have already discussed:
365 *Delta proteobacteria* ASV1 (ORM2), two *Ca. Nealsonbacteria* ASVs (OD1) and *Ca. Omnitrophica* ASV1
366 (Figures S6a and S6b). High abundance ASVs associated with *Methanosaeta* and *Methanoregula* also
367 decreased 1-2 orders of magnitude follow the addition of 10 mL air (Figures S7a and S7b).

368 Concentrations of most of these bacterial and archaeal ASVs did not begin to recover until after ORM2
369 growth resumed and methanogenic benzene degradation was re-established. Notably, a few Group 2
370 ASVs in Bottles 1 and 2 never fully recovered from O₂ exposure, including *Ca. Nealsonbacteria* ASV1
371 (Figures S6a and S6b), *Methanoregula* ASV2 and *Methanosaeta* ASV4 (Figures S7a and S7b), pointing to
372 likely permanent community impacts.

373

374 Group 3 comprises largely unimpacted microbes that were in low abundance and include two
375 unclassified *Spirochaetaceae* ASVs, one ASV belonging to an unclassified *Anaerolineaceae* genus, and
376 one ASV belonging to hydrogenotrophic *Methanobacterium* (Figures S6a – S6d and S7a – S7d).
377 *Spirochaetaceae* and *Anaerolineaceae* are commonly detected in anaerobic and methanogenic
378 hydrocarbon-degrading enrichment cultures, but their roles often undefined. Some Spirochaetes are
379 believed to mediate recycling of biomass from dead cells (Dong et al., 2018). *Anaerolineaceae* are often
380 closely associated with methanogens and may catalyze the degradation of other hydrocarbons (Liang et
381 al., 2015; Mohamad Shahimin and Siddique, 2017). Our results suggest that the roles of Group 3
382 microorganisms are independent of benzene degradation.

383

384 **Implications for the field.** This study has made it abundantly clear that ORM2, the chief anaerobic
385 benzene degrader in the DGG-B/OR consortium, is strictly anaerobic and oxygen-sensitive. Transient
386 oxygen exposure contributed to extensive, prolonged decay of ORM2 and associated Group 2
387 methanogens and putative biomass-recycling bacteria. A complete (closed) genome for ORM2 has been
388 sequenced and is under investigation (JGI/IMG taxon ID 2795385393) but its biochemical mechanism for
389 benzene transformation is still not known. Nevertheless, we can say for certain is that oxygen is not

390 involved in anaerobic benzene degradation by this culture and probably not in other consortia harboring
391 ORM2-like benzene degraders (Sakai et al., 2009; Noguchi et al., 2014; Qiao et al., 2018).

392
393 For years our laboratory has wondered why anaerobic benzene degraders such as ORM2 rarely
394 proliferate in subsurface benzene-contaminated environments. We recently explored environmental co-
395 contaminants (*i.e.*, toluene and xylenes) and microbial co-dependencies as possibilities constraining
396 their growth (Toth et al., 2021) but acknowledged that a multitude of other factors were likely involved.
397 This study implicates transient oxygen exposure as another possibility. In the subsurface, dissolved
398 oxygen may be introduced to anoxic zones from groundwater recharge, fluctuations in groundwater
399 elevation, rain events, and diffusion from the vadose zone. Shallow unconfined aquifers are much more
400 likely to see oxygen incursions. However, unlike our culture bottles, subsurface environments are highly
401 heterogeneous and filled with microenvironments that would not see bulk oxygen concentrations.
402 Nevertheless, careful attention to avoiding changes in redox potential appears warranted if sustained
403 anaerobic benzene biotransformation is desired.

404
405 This study has also highlighted pronounced cell death/decay as another important factor constraining
406 net microbial growth. Cell decay is often ignored in mathematical models, particularly in contaminant
407 fate and transport models. It is frequently assumed that because anaerobic bacteria do not grow
408 quickly, their decay rates must also be very low and can therefore be neglected. A rule of thumb is that
409 decay rates are 1/10th of growth rates (Rittmann and McCarty, 2001). Contrarily, we observed for ORM2
410 that growth and decay rates were of similar magnitude, even when oxygen was no longer present. This
411 result is consistent with previously described challenges in achieving high cell densities and consistent
412 benzene degradation rates in lab cultures. They could also help explain why organisms putatively
413 associated with biomass recycling, including *Ca. Nealsonbacteria* (OD1) and *Ca. Omnitrophica* (OP3),
414 among others, are periodically observed in high abundances in the DGG-B/OR consortium (Luo et al.,
415 2016; Toth et al., 2021) and other anaerobic benzene-degrading consortia (Taubert et al., 2012;
416 Melkonian et al., 2021). What factors could explain such relatively high decay rates? Possible
417 explanations include viral and bacterial predation or microbial competition. Another explanation could
418 be the formation of toxic reactive intermediates during benzene activation resulting in cell death, or the
419 energy penalty afforded by this difficult reaction. Understanding the underlying mechanisms of death
420 and decay will be key to establishing more robust cultures for bioremediation. Interestingly, comparable
421 methanogenic enrichment cultures that degrade toluene rather than benzene do not exhibit the same
422 struggles and thus the most likely hypothesis is that a step in the biochemical activation of benzene
423 contributes to higher rates of decay.

424
425 **AUTHOR CONTRIBUTIONS**
426 All authors made research and substantial intellectual contributions to the completion of this study.
427 E.A.E., S.G. and F.L. conceived the project. S.G. established all experimental bottles and performed all GC
428 measurements, DNA extractions and qPCR assays, with assistance from X.C. and J.X. Amplicon
429 sequencing data processing and analyses were completed by S.G. and C.R.A.T. Cell yields, growth and
430 decay rate estimates were completed by C.R.A.T., S.G., and E.A.E. The manuscript was written by S.G.,
431 C.R.A.T. and E.A.E. All authors contributed to manuscript revision and have approved the submitted
432 version.

433
434 **SUPPORTING INFORMATION**
435 Figures showing benzene and methane concentrations and microbial profiles in Bottle 5 (positive
436 control), Bottle 1 (oxygen-amended), Bottle 3 (oxygen-amended) and Bottle 6 (sterile) over time;

437 maximum likelihood consensus tree for *Pseudomonas*; absolute abundance of specific bacterial and
438 archaeal groups in all bottles ([PDF](#))

439 Primers used for amplification; benzene and methane concentrations; qPCR raw data including
440 calibration curves; all gDNA samples sequenced, including ASVs and their taxonomic assignment;
441 calculation of absolute abundances; oxygen demand stoichiometry; estimation of yields, growth and
442 decay rates ([XLSX](#))

443

444 **ACKNOWLEDGEMENTS**

445 This study was funded by Genomic Application Partnership Program (GAPP) grants awarded to E.A.E.
446 (Project IDs OGI-102 and OGI-173), which were supported by Genome Canada, Ontario Genomics, the
447 Government of Ontario, Mitacs Canada, SiREM, Alberta Innovates, Federated Co-operatives Limited, and
448 Imperial Oil. The authors would like to thank SiREM (Guelph, Ontario N1G 3Z2, Canada) for supplying
449 DGG-B culture for oxygen tolerance testing. We would also like to acknowledge the laboratories of Dr.
450 Neil Thomson (University of Waterloo), Dr. Ania Ulrich (University of Alberta), SiREM, and Innotech
451 Alberta (Edmonton, Alberta T6N 1E4, Canada) for providing feedback and intellectual contributions to
452 this study during weekly GAPP consortium meetings.

453

454

455 **REFERENCES**

456 Abu Laban, N., Selesi, D., Rattei, T., Tischler, P., and Meckenstock, R.U. (2010). Identification of enzymes
457 involved in anaerobic benzene degradation by a strictly anaerobic iron-reducing enrichment
458 culture. *Environ Microbiol* 12, 2783-2796. doi: 10.1111/j.1462-2920.2010.02248.x.

459 Atashgahi, S., Hornung, B., van der Waals, M.J., da Rocha, U.N., Hugenholtz, F., Nijssse, B., et al. (2018). A
460 benzene-degrading nitrate-reducing microbial consortium displays aerobic and anaerobic
461 benzene degradation pathways. *Sci. Rep.* 8, 4490. doi: 10.1038/s41598-018-22617-x.

462 Atlas, R.M. (1981). Microbial Degradation of Petroleum Hydrocarbons: an Environmental Perspective.
463 *Microbiol Rev* 45(1), 180-209.

464 Bruce, R.A., Achenbach, L.A., and Coates, J.D. (1999). Reduction of (per)chlorate by a novel organism
465 isolated from paper mill waste. *Environ Microbiol* 1(4), 319-329.

466 Burland, S.M., and Edwards, E.A. (1999). Anaerobic benzene biodegradation linked to nitrate reduction.
467 *Appl. Environ. Microbiol.* 65, 529-533.

468 Caldwell, M.E., and Sufliita, J.M. (2000). Detection of Phenol and Benzoate as Intermediates of Anaerobic
469 Benzene Biodegradation under Different Terminal Electron-Accepting Conditions. *Environ Sci
470 Technol* 34, 1216-1220.

471 Callahan, B.J., McMurdie, P.J., Rosen, M.J., Han, A.W., Johnson, A.J., and Holmes, S.P. (2016). DADA2:
472 High-resolution sample inference from Illumina amplicon data. *Nat Methods* 13(7), 581-583. doi:
473 10.1038/nmeth.3869.

474 Chakraborty, R., O'Connor, S.M., Chan, E., and Coates, J.D. (2005). Anaerobic degradation of benzene,
475 toluene, ethylbenzene, and xylene compounds by Dechloromonas strain RCB. *Appl Environ
476 Microbiol* 71(12), 8649-8655. doi: 10.1128/AEM.71.12.8649-8655.2005.

477 Coates, J.D., Anderson, R.T., Woodwards, J.C., Phillips, E.J.P., and Lovley, D.R. (1996). Anaerobic
478 hydrocarbon degradation in petroleum-contaminated harbor sediments under sulfate-reducing
479 and artificially imposed iron-reducing conditions. *Environ Sci Technol* 30, 2784-2789.

480 Cunningham, J.A., Rahme, H., Hopkins, G.D., Lebron, C., and Reinhard, M. (2001). Enhanced in situ
481 bioremediation of BTEX-contaminated groundwater by combined injection of nitrate and
482 sulfate. *Environ. Sci. Technol.* 35, 1663-1670.

483 Devine, C.E. (2013). *Identification of key organisms, genes and pathways in benzene-degrading*
484 *methanogenic cultures*. Doctor of Philosophy, University of Toronto.

485 Dong, X., Greening, C., Bruls, T., Conrad, R., Guo, K., Blaskowski, S., et al. (2018). Fermentative
486 Spirochaetes mediate necromass recycling in anoxic hydrocarbon-contaminated habitats. *ISME*
487 *J.* 12, 2039-2050. doi: 10.1038/s41396-018-0148-3.

488 Edwards, E.A., and Grbić-Galić, D. (1992). Complete mineralization of benzene by aquifer
489 microorganisms under strictly anaerobic conditions. *Appl. Environ. Microbiol.* 58, 2663-2666.

490 Ettwig, K.F., Butler, M.K., Le Paslier, D., Pelletier, E., Mangenot, S., Kuyper, M.M., et al. (2010). Nitrite-
491 driven anaerobic methane oxidation by oxygenic bacteria. *Nature* 464(7288), 543-548. doi:
492 10.1038/nature08883.

493 Galdames, A., Ruiz-Rubio, L., Orueta, M., Sanchez-Arzalluz, M., and Vilas-Vilela, J.L. (2020). Zero-Valent
494 Iron Nanoparticles for Soil and Groundwater Remediation. *Int J Environ Res Public Health* 17(16).
495 doi: 10.3390/ijerph17165817.

496 Grbić-Galić, D., and Vogel, T.M. (1987). Transformation of toluene and benzene by mixed methanogenic
497 cultures. *Appl Environ Microbiol* 53(2), 254-260.

498 Grimberg, S.J., Stringfellow, W.T., and Aitken, M.D. (1996). Quantifying the biodegradation of
499 phenanthrene by *Pseudomonas stutzeri* P16 in the presence of a nonionic surfactant. *Appl*
500 *Environ Microbiol* 62(7), 2387-2392.

501 Heinaru, E., Naanuri, E., Grunbach, M., Joesaar, M., and Heinaru, A. (2016). Functional redundancy in
502 phenol and toluene degradation in *Pseudomonas stutzeri* strains isolated from the Baltic Sea.
503 *Gene* 589(1), 90-98. doi: 10.1016/j.gene.2016.05.022.

504 Holmes, D.E., Risso, C., Smith, J.A., and Lovley, D.R. (2011). Anaerobic oxidation of benzene by the
505 hyperthermophilic archaeon *Ferroglobus placidus*. *Appl. Environ. Microbiol.* 77(17), 5926-5933.
506 doi: 10.1128/AEM.05452-11.

507 Kazumi, J., Caldwell, M.E., Suflita, J.M., Lovley, D.R., and Young, L.Y. (1997). Anaerobic Degradation of
508 Benzene in Diverse Anoxic Environments. *Environ Sci Technol* 31, 813-818.

509 Kralik, P., and Ricchi, M. (2017). A Basic Guide to Real Time PCR in Microbial Diagnostics: Definitions,
510 Parameters, and Everything. *Front Microbiol* 8, 108. doi: 10.3389/fmicb.2017.00108.

511 Kunapuli, U., Griebler, C., Beller, H.R., and Meckenstock, R.U. (2008). Identification of intermediates
512 formed during anaerobic benzene degradation by an iron-reducing enrichment culture. *Environ*
513 *Microbiol* 10(7), 1703-1712. doi: 10.1111/j.1462-2920.2008.01588.x.

514 Lalucat, J., Bennasar, A., Bosch, R., Garcia-Valdes, E., and Palleroni, N.J. (2006). Biology of *Pseudomonas*
515 *stutzeri*. *Microbiol Mol Biol Rev* 70(2), 510-547. doi: 10.1128/MMBR.00047-05.

516 Liang, B., Wang, L.Y., Mbadinga, S.M., Liu, J.F., Yang, S.Z., Gu, J.D., et al. (2015). *Anaerolineaceae* and
517 *Methanosaeta* turned to be the dominant microorganisms in alkanes-dependent methanogenic
518 culture after long-term of incubation. *AMB Express* 5(1), 117. doi: 10.1186/s13568-015-0117-4.

519 Löffler, F.E., and Edwards, E.A. (2006). Harnessing microbial activities for environmental cleanup. *Curr*
520 *Opin Biotechnol* 17(3), 274-284. doi: 10.1016/j.copbio.2006.05.001.

521 Lovley, D.R., Coates, J.D., Woodward, J.C., and Phillips, E.J.P. (1995). Benzene oxidation coupled to
522 sulfate reduction. *Appl Environ Microbiol* 61(3), 953-958.

523 Lu, S., Zhang, X., and Xue, Y. (2017). Application of calcium peroxide in water and soil treatment: A
524 review. *J Hazard Mater* 337, 163-177. doi: 10.1016/j.jhazmat.2017.04.064.

525 Luo, F., Devine, C.E., and Edwards, E.A. (2016). Cultivating microbial dark matter in benzene-degrading
526 methanogenic consortia. *Environ. Microbiol.* 18, 2923-2936. doi: 10.1111/1462-2920.13121.

527 Luo, F., Gitiafroz, R., Devine, C.E., Gong, Y., Hug, L.A., Raskin, L., et al. (2014). Metatranscriptome of an
528 anaerobic benzene-degrading, nitrate-reducing enrichment culture reveals involvement of
529 carboxylation in benzene ring activation. *Appl. Environ. Microbiol.* 80, 4095-4107. doi:
530 10.1128/AEM.00717-14.

531 Major, D.W., McMaster, M.L., Cox, E.E., Edwards, E.A., Dworatzek, S.M., Hendrickson, E.R., et al. (2002).
532 Field demonstration of successful bioaugmentation to achieve dechlorination of
533 tetrachloroethane to ethane. *Environ Sci Technol* 36, 5106-5116.

534 Mancini, S.A., Devine, C.E., Elsner, M., Nandi, M.E., Ulrich, A.C., Edwards, E.A., et al. (2008). Isotopic
535 evidence suggests different initial reaction mechanisms for anaerobic benzene biodegradation.
536 *Environ Sci Technol* 42, 8290-8296.

537 Meckenstock, R.U., Boll, M., Mouttaki, H., Koelschbach, J.S., Cunha Tarouco, P., Weyrauch, P., et al.
538 (2016). Anaerobic Degradation of Benzene and Polycyclic Aromatic Hydrocarbons. *J Mol*
539 *Microbiol Biotechnol* 26(1-3), 92-118. doi: 10.1159/000441358.

540 Mehboob, F., Junca, H., Schraa, G., and Stams, A.J. (2009). Growth of *Pseudomonas chloritidismutans*
541 AW-1(T) on n-alkanes with chlorate as electron acceptor. *Appl Microbiol Biotechnol* 83(4), 739-
542 747. doi: 10.1007/s00253-009-1985-9.

543 Melkonian, C., Fillinger, L., Atashgahi, S., da Rocha, U.N., Kuiper, E., Olivier, B., et al. (2021). High
544 biodiversity in a benzene-degrading nitrate-reducing culture is sustained by a few primary
545 consumers. *Commun Biol* 4(1), 530. doi: 10.1038/s42003-021-01948-y.

546 Mohamad Shahimin, M.F., and Siddique, T. (2017). Sequential biodegradation of complex naphtha
547 hydrocarbons under methanogenic conditions in two different oil sands tailings. *Environ Pollut*
548 221, 398-406. doi: 10.1016/j.envpol.2016.12.002.

549 Nales, M., Butler, B.J., and Edwards, E.A. (1998). Anaerobic benzene biodegradation: A microcosm
550 survey. *Bioremediat. J.* 2, 125-144. doi: 10.1080/10889869891214268.

551 Noguchi, M., Kurisu, F., Kasuga, I., and Furumai, H. (2014). Time-resolved DNA stable isotope probing
552 links *Desulfobacterales*- and *Coriobacteriaceae*-related bacteria to anaerobic degradation of
553 benzene under methanogenic conditions. *Microbes Environ.* 29, 191-199. doi:
554 10.1264/jmse2.ME13104.

555 Oosterkamp, M.J., Veuskens, T., Talarico Saia, F., Weelink, S.A., Goodwin, L.A., Daligault, H.E., et al.
556 (2013). Genome analysis and physiological comparison of *Alicycliphilus denitrificans* strains BC
557 and K601(T.). *PLoS One* 8(6), e66971. doi: 10.1371/journal.pone.0066971.

558 Ortega-Calvo, J.J., Marchenko, A.I., Vorobyov, A.V., and Borovick, R.V. (2003). Chemotaxis in polycyclic
559 aromatic hydrocarbon-degrading bacteria isolated from coal-tar- and oil-polluted rhizospheres.
560 *FEMS Microbiology Ecology* 44(3), 373-381. doi: 10.1016/s0168-6496(03)00092-8.

561 Otto, M., Floyd, M., and Bajpai, S. (2008). Nanotechnology for site remediation. *Remediation Journal*
562 19(1), 99-108. doi: 10.1002/rem.20194.

563 Phelps, C.D., Kazumi, J., and Young, L.Y. (1996). Anaerobic degradation of benzene in BTX mixtures
564 dependent on sulfate reduction. *FEMS Microbiol Lett* 145, 433-437.

565 Qiao, W., Luo, F., Lomheim, L., Mack, E.E., Ye, S., Wu, J., et al. (2018). Natural attenuation and anaerobic
566 benzene detoxification processes at a chlorobenzene-contaminated industrial site inferred from
567 field investigations and microcosm studies. *Environ. Sci. Technol.* 52, 22-31. doi:
568 10.1021/acs.est.7b04145.

569 Quast, C., Pruesse, E., Yilmaz, P., Gerken, J., Schweer, T., Yarza, P., et al. (2013). The SILVA ribosomal RNA
570 gene database project: improved data processing and web-based tools. *Nucleic Acids Res.* 41,
571 D590-D596. doi: 10.1093/nar/gks1219.

572 Reinhard, M., Shang, S., Kitanidis, P.K., Orwin, E., Hopkins, G.D., and Lebron, C.A. (1997). In situ BTEX
573 biotransformation under enhanced nitrate- and sulfate-reducing conditions. *Environ. Sci.*
574 *Technol.* 31, 28-36.

575 Rittmann, B.E., and McCarty, P.L. (2001). *Environmental biotechnology: principles and applications*. New
576 York: McGraw-Hill.

577 Sakai, N., Kurisu, F., Yagi, O., Nakajima, F., and Yamamoto, K. (2009). Identification of putative benzene-
578 degrading bacteria in methanogenic enrichment cultures. *J. Biosci. Bioeng.* 108, 501-507. doi:
579 10.1016/j.jbiosc.2009.06.005.

580 Suominen, S., Dombrowski, N., Sinninghe Damste, J.S., and Villanueva, L. (2021). A diverse uncultivated
581 microbial community is responsible for organic matter degradation in the Black Sea sulphidic
582 zone. *Environ Microbiol* 23(6), 2709-2728. doi: 10.1111/1462-2920.14902.

583 Taubert, M., Vogt, C., Wubet, T., Kleinsteuber, S., Tarkka, M.T., Harms, H., et al. (2012). Protein-SIP
584 enables time-resolved analysis of the carbon flux in a sulfate-reducing, benzene-degrading
585 microbial consortium. *ISME J* 6(12), 2291-2301. doi: 10.1038/ismej.2012.68.

586 Toth, C.R.A., Luo, F., Bawa, N., Webb, J., Guo, S., Dworatzek, S., et al. (2021). Anaerobic Benzene
587 Biodegradation Linked to the Growth of Highly Specific Bacterial Clades. *Environ Sci Technol*
588 55(12), 7970-7980. doi: 10.1021/acs.est.1c00508.

589 Ulrich, A.C., and Edwards, E.A. (2003). Physiological and molecular characterization of anaerobic
590 benzene-degrading mixed cultures. *Environ. Microbiol.* 5, 92-102.

591 Vela, S., Häggblom, M.M., and Young, L.Y. (2002). Biodegradation of aromatic and aliphatic compounds
592 by rhizobial species. *Soil Sci* 167(12), 802-810. doi: 10.1097/01.ss.0000043034.84859.0a.

593 Vogel, T.M., and Grbić-Galić, D. (1986). Incorporation of oxygen from water into toluene and benzene
594 during anaerobic fermentative transformation. *Appl Environ Microbiol* 52(1), 200-202.

595 Vogt, C., Kleinsteuber, S., and Richnow, H.H. (2011). Anaerobic benzene degradation by bacteria. *Microb
596 Biotechnol* 4(6), 710-724. doi: 10.1111/j.1751-7915.2011.00260.x.

597 Ward, D.M., Atlas, R.M., Boehm, P.D., and Calder, A. (1980). Microbial biodegradation and chemical
598 evolution of oil from the Amoco spill. *Ambio* 9(6), 277-283.

599 Watanabe, T., Kojima, H., and Fukui, M. (2015). *Sulfuriferula multivorans* gen. nov., sp. nov., isolated
600 from a freshwater lake, reclassification of '*Thiobacillus plumbophilus*' as *Sulfuriferula
601 plumbophilus* sp. nov., and description of *Sulfuricellaceae* fam. nov. and *Sulfuricellales* ord. nov.
602 *Int J Syst Evol Microbiol* 65(Pt 5), 1504-1508. doi: 10.1099/ijsem.0.000129.

603 Watanabe, T., Kojima, H., and Fukui, M. (2016). *Sulfuriferula thiophila* sp. nov., a chemolithoautotrophic
604 sulfur-oxidizing bacterium, and correction of the name *Sulfuriferula plumbophilus* Watanabe,
605 Kojima and Fukui 2015 to *Sulfuriferula plumbiphila* corrig. *Int J Syst Evol Microbiol* 66(5), 2041-
606 2045. doi: 10.1099/ijsem.0.000988.

607 Weelink, S.A., Tan, N.C., ten Broeke, H., van den Kieboom, C., van Doesburg, W., Langenhoff, A.A., et al.
608 (2008). Isolation and characterization of *Alicycliphilus denitrificans* strain BC, which grows on
609 benzene with chlorate as the electron acceptor. *Appl Environ Microbiol* 74(21), 6672-6681. doi:
610 10.1128/AEM.00835-08.

611 Weiner, J.M., and Lovley, D.R. (1998). Rapid benzene degradation in methanogenic sediments from a
612 petroleum-contaminated aquifer. *Appl Environ Microbiol* 64(5), 1937-1939.

613 Wilson, B.H., Smith, G.B., and Rees, J.F. (1986). Biotransformation of selected alkylbenzenes and
614 halogenated aliphatic hydrocarbons in methanogenic aquifer material: a microcosm study.
615 *Environ Sci Technol* 20, 997-1002.

616 Zhang, T., Tremblay, P.L., Chaurasia, A.K., Smith, J.A., Bain, T.S., and Lovley, D.R. (2013). Anaerobic
617 benzene oxidation via phenol in *Geobacter metallireducens*. *Appl. Environ. Microbiol.* 79, 7800-
618 7806. doi: 10.1128/AEM.03134-13.

619

Table 1. Layout of experimental treatments and overview of results

Bottle number ^a	First air addition ^b (0.1 mL)	Second air addition ^b (10 mL)	Third air addition ^b (14 mL)	Days when resazurin was pink (aerobic)	Day methanogenic benzene degradation recovered
Bottle 1	Day 39	Day 94	None	94 – 155 (61 d)	After Day 477
Bottle 2	Day 53	Day 94	Day 224	94 – 164 (70 d); 224 – 259 (35 d)	After Day 583
Bottle 3	Day 39	None	None	0	Recovered immediately
Bottle 4	None	None	None	0	N/A; Anoxic Control
Bottle 5	None	None	None	0	N/A; Anoxic Control
Bottle 6	Day 16	None	None	16 – 155 (stayed pink)	N/A; Sterile Control

^aBottles were 40 mL screwcap vials containing 30 mL liquid and 10 mL headspace. Bottles were sealed with Teflon Mininert caps.

^bSmall injections of 0.1 mL air were carried out using a sterile syringe inside the anaerobic glove box. Larger (10-14 mL) additions of air were achieved by removing bottles from the glove box and opening the cap for 15 s, then closing the cap and immediately returning bottles to the glovebox.

N/A: not applicable.

Table 2. Estimated first order growth and decay rates for benzene-degrading microorganisms in DGG-B.

Parameter ^{a,b,c}	<i>Pseudomonas</i> ASV1	ORM2
	Growth: Aerobic	Growth: Anaerobic
	Decay: Anaerobic	Decay: Aerobic
Average 1 st order growth rate (day ⁻¹)	0.079 ± 0.02 (n=4)	0.011 ± 0.002 (n=5)
Average doubling time (days)	8.7	66
Fastest 1 st order growth rate (day ⁻¹)	0.11	0.03
Shortest doubling time (days)	6.4	26
Average net yield (g cells/g benzene)	1.1 ± 0.3 (n=4)	0.039 ± 0.010 (n=15) ^d
Theoretical growth yield (g cells/g benzene)	1.1	0.22
Average 1 st order decay rate (day ⁻¹)	-0.006 ± 0.000 (n=2)	-0.018 ± 0.006 (n=5)
Average half-life (days)	116	38
Fastest 1 st order decay rate (day ⁻¹)	-0.018	-0.07
Shortest half-life (days)	39	11

^aAverage and max/min rates were estimated using log-linear regression of qPCR data (cell concentration) over time during periods of net growth or decay as detailed in Table S8.

^bYields were calculated for time intervals where significant growth was observed (see Table S8 for calculations).

^cStandard errors are shown when n > 2. If n=2, error is equal to range/2.

^dYield shown is sum of the yield of ORM2 plus yield of Archaea for comparison to stoichiometric equation (i.e., total biomass).

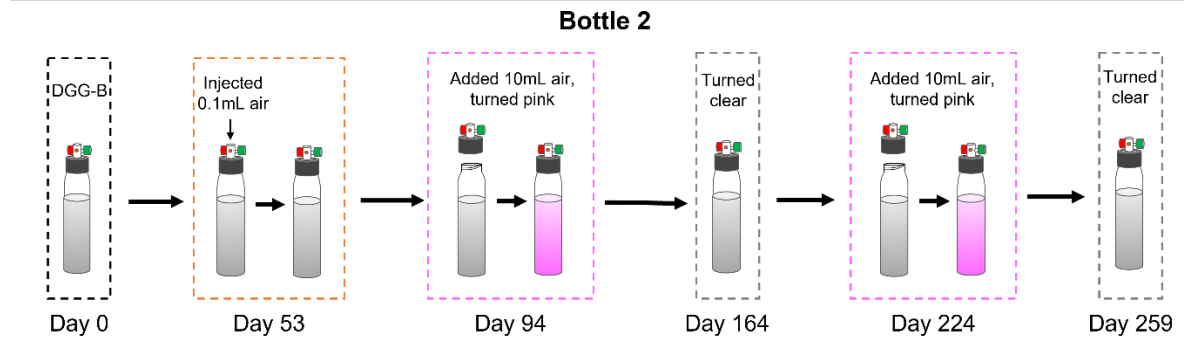


Figure 1. Illustration of oxygen treatment performed with DGG-B culture in Bottle 2.

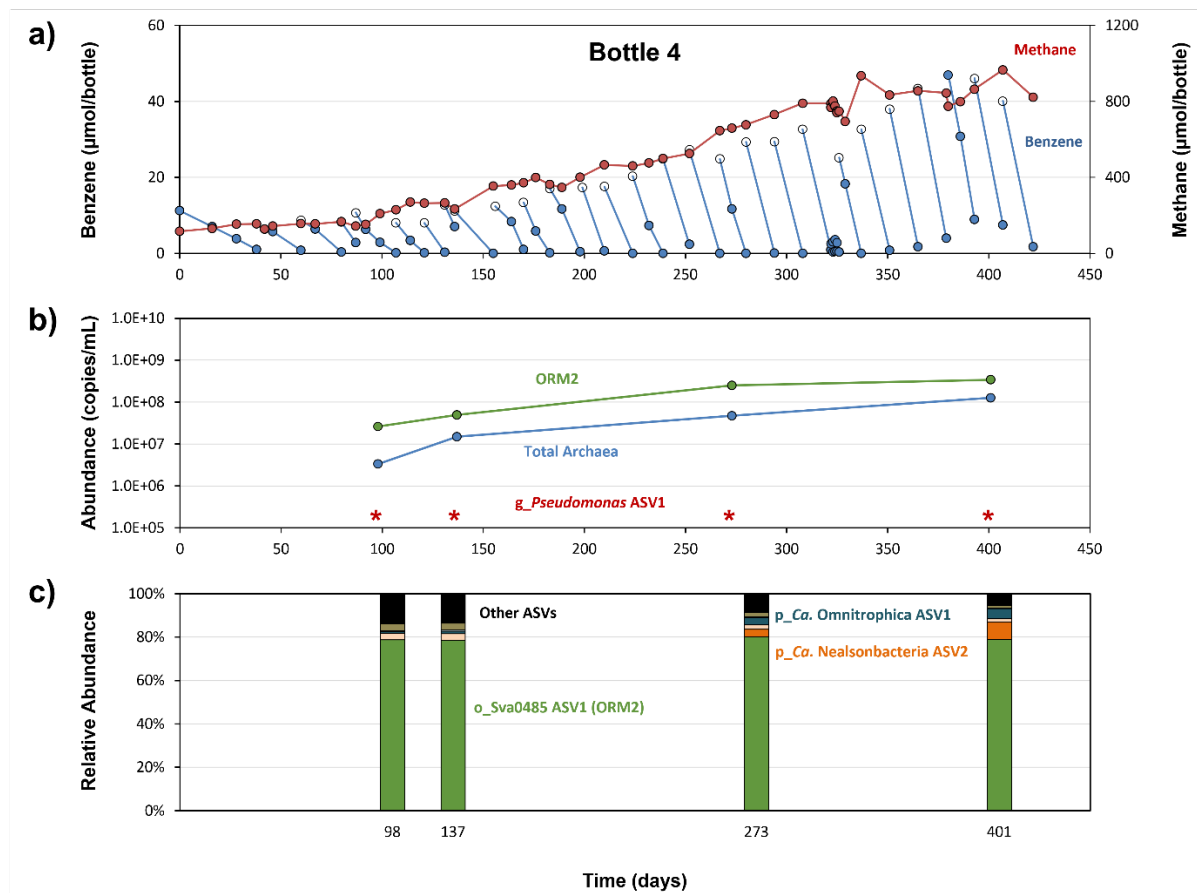


Figure 2. Benzene and methane concentrations and microbial profiles in anoxic control **Bottle 4 over time.** Panel a) presents benzene depletion (blue) and methane production (red) measured by GC-FID, where closed circles denote measured concentrations while open circles are expected benzene concentrations based on the amount fed. The center panel b) shows the absolute abundances of targeted 16S rRNA gene copies. ORM2 and Total Archaea were analyzed by qPCR; abundance of *Pseudomonas* ASV1 was calculated based on the total Bacteria qPCR abundance (Table S3) multiplied by relative abundance obtained from amplicon sequencing (Table S5). Abundances below quantifiable limits are designated by stars (*). The bottom panel c) summarizes the relative bacterial community composition measured in the bottle.

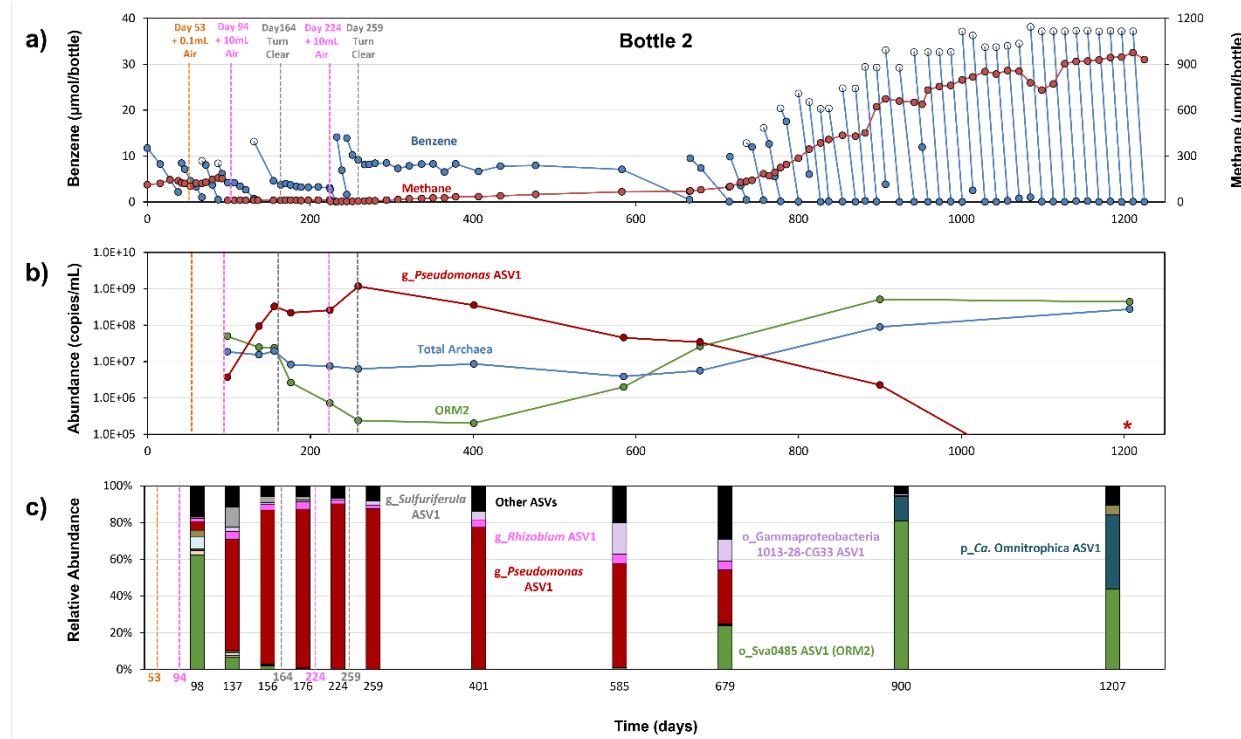


Figure 3. Benzene and methane concentrations and microbial profiles in oxygen-exposed Bottle 2 over time. Panel a) presents benzene depletion (blue) and methane production (red) measured by GC-FID, where closed circles denote measured concentrations while open circles are expected benzene concentrations based on the amount fed. The center panel b) shows the absolute abundances of targeted 16S rRNA gene copies. ORM2 and Total Archaea were analyzed by qPCR; abundance of *Pseudomonas* ASV1 was calculated based on the total Bacteria qPCR abundance (Table S3) multiplied by relative abundance obtained from amplicon sequencing (Table S5). Abundances below quantifiable limits are designated by stars (*). The bottom panel c) summarizes the relative bacterial community composition measured in the bottle.